Polar Biol (2010) 33:1599–1614
DOI 10.1007/s00300-010-0806-z

ORIGINAL PAPER

Variability of the microbial community in the western Antarctic Peninsula from late fall to spring during a low ice cover year

Sébastien Moreau · Gustavo A. Ferreyra · Bernard Mercier · Karine Lemarchand · Marie Lionard · Suzanne Roy · Behzad Mostajir · Sébastien Roy · Bon van Hardenberg · Serge Demers

Received: 27 October 2009 / Revised: 8 March 2010 / Accepted: 26 April 2010 / Published online: 20 May 2010

Abstract Although winter conditions play a major role in determining the productivity of the western Antarctic Peninsula (WAP) waters for the following spring and summer, a few studies have dealt with the seasonal variability of microorganisms in the WAP in winter. Moreover, because of regional warming, sea-ice retreat is happening earlier in spring, at the onset of the production season. In this context, this study describes the dynamics of the marine microbial community in the Melchior Archipelago (WAP) from fall to spring 2006. Samples were collected monthly to biweekly at four depths from the surface to the aphotic layer. The abundance and carbon content of bacteria, phytoplankton and microzooplankton were analyzed using flow cytometry and inverted microscopy, and bacterial richness was examined by PCR–DGGE. As expected, due to the extreme environmental conditions, the microbial community abundance and biomass were low in fall and winter. Bacterial abundance ranged from 1.2 to 2.8 × 10^5 cells ml^{-1} showing a slight increase in spring. Phytoplankton biomass was low and dominated by small cells (<2 μm) in fall and winter (average chlorophyll *a* concentration, Chl-*a*, of, respectively, 0.3 and 0.13 μg l^{-1}). Phytoplankton biomass increased in spring (Chl-*a* up to 1.13 μg l^{-1}), and, despite potentially adequate growth conditions, this rise was small and phytoplankton was still dominated by small cells (2–20 μm). In addition, the early disappearing of sea-ice in spring 2006 let the surface water exposed to ultraviolet B radiations (UVBR, 280–320 nm), which seemed to have a negative impact on the microbial community in surface waters.

Keywords Microbial food web · Antarctica · Sea-ice · Ozone hole · UV radiations

S. Moreau (✉) · G. A. Ferreyra · B. Mercier · K. Lemarchand · M. Lionard · Suzanne Roy · Sébastien Roy · S. Demers
Institut des sciences de la mer de Rimouski (ISMER), Université du Québec à Rimouski, 310 allée des Ursulines, Rimouski, Québec G5L 3A1, Canada
e-mail: sebastien.moreau@uqar.qc.ca

G. A. Ferreyra
Instituto Antártico Argentino, Cerrito 1248 (1010), Buenos Aires, Argentina

B. van Hardenberg
Department of Fisheries and Oceans, Institute of Ocean Sciences, 9860 West Saanich Road, Sidney, BC V8L 4B, Canada

B. Mostajir
Laboratoire Écosystèmes Lagunaires, UMR 5119 (Université Montpellier 2, CNRS, IFREMER, IRD), Case 093, 34095 Montpellier Cedex 05, France

Introduction

The Southern Ocean, and hence the WAP waters, undergo extreme seasonal fluctuations in terms of light regime, sea-ice concentration and productivity (Delille 2004). However, most oceanographic studies in the WAP have taken place during the more productive periods (i.e. late spring–early summer) when strong phytoplankton blooms occur (e.g. Smith et al. 2008; Vernet et al. 2008; Reiss et al. 2009). Indeed, a few studies have dealt with the seasonal variability of microorganisms in the WAP through winter, and these studies focused on the distribution and diversity of bacterioplankton (Murray et al. 1998; Church et al. 2003), microzooplankton grazing and phytoplankton growth (Brightman and Smith 1989; Pearce et al. 2008) and the distribution of krill (Lawson et al. 2004). This is attributable to very difficult sampling conditions during

winter and to a specific interest in highly productive periods. Nevertheless, because winter conditions will in part determine the production for the following spring and summer, winter studies are necessary. Indeed, winter sea-ice conditions are a major determinant of the productivity of WAP waters during the subsequent spring and summer (Smith et al. 1998; Smith et al. 2001). Poor winter sea-ice conditions may also favor the presence of salps, which have a low nutritive value for higher predators, over krill, which represent a major link to higher trophic levels in the WAP (Siegel and Loeb 1995; Loeb et al. 1997).

Because of global warming and seasonal stratospheric ozone layer breakdown, the WAP is subjected to changing environmental conditions, and more particularly, during winter and spring. The "ozone hole", which refers to a strong reduction in the concentration of stratospheric ozone, has been observed every spring over Antarctica for the last 20 years (McKenzie et al. 2007). In consequence, the intensities of UVBR reaching the surface of the Southern Ocean have increased (Arrigo 1994; Frederick and Lubin 1994). On the other hand, the WAP has experienced a significant rise in air temperatures during the last 50 years (+0.56°C per decade; Marshall et al. 2002). This rise was important mostly in winter (+1.09°C per decade; Turner et al. 2005) and coincided with a decrease in the duration of sea-ice cover and more particularly an earlier retreat of sea-ice (Stammerjohn et al. 2008). As a consequence, sea-ice retreat may now coincide with the seasonally occurring ozone hole and lead to potentially harmful conditions where no or low ice cover can shield the water column from harmful UVBR (Cockell and Córdoba-Jabonero 2004; Lesser et al. 2004).

UVBR and ultraviolet A radiation (UVAR, 320–400 nm) are recognized to have significant impacts on marine organisms, including DNA damage (Häder and Sinha 2005) and photoinhibition (e.g. Cullen et al. 1992; Neale et al. 1998). These radiations may also affect indirectly the microbial community through trophic interactions (Mostajir et al. 1999; Davidson and Belbin 2002; Ferreyra et al. 2006). On the other hand, global warming may have both positive and negative effects on the microbial community of the WAP. Higher temperatures should promote higher growth and photosynthesis rates and should favor enzyme-based photorepair mechanisms (Bouchard et al. 2006). Moreover, the predicted earlier retreat of sea-ice in the WAP may lead to a longer growth season, as long as nutrients are available. Under this assumption, it has been hypothesized that overall plankton biomass will be higher in the future for the Southern Ocean (Arrigo and Thomas 2004; Sarmiento et al. 2004) as it has already been modeled for the Arctic Ocean (Arrigo et al. 2008). However, by changing the dynamics of sea-ice and water column stratification, global warming might also have negative effects on the microbial community of the WAP (Sarmiento et al. 2004; Häder et al. 2007). Finally, earlier ice melting due to global warming may expose the growing phytoplankton populations to high UVBR during the ozone hole period (Häder et al. 2007).

The present study was conducted in the WAP over the 2006 austral late-fall, winter and early-spring seasons in the Scholaert Channel, in the vicinity of the Melchior Archipelago. The aim of this research was to study the dynamics of the microbial community during this time of the year when productivity is minimum (late fall and winter) and at the onset of the production season (early spring) when the ozone hole may threaten the WAP microbial community.

Materials and methods

Sampling

This project was undertaken in a shallow bay (maximum depth of 150 m) of the Melchior Archipelago (Scholaert Channel) in the WAP (Fig. 1), where the Sedna IV sailboat wintered from June 3rd to November 10th 2006. A GUV-510 surface spectral radiometer (Biospherical Instruments Inc., USA; later on abbreviated as GUV) was fixed on the Sedna IV boat at a shadow-free site to monitor incident UVBR, UVAR and photosynthetically available radiation (PAR, 400–700 nm) every 15 min during the whole study period. Sampling was performed aboard rubber boats at a fixed station (64°19′31″S, 62°53′42″W) located ~1 km from the coast. Vertical profiles of water column characteristics were obtained using a Conductivity, Temperature and Depth data logger (CTD; model SBE 19 Plus, Sea-Bird Electronics, Inc.) equipped with a fluorescence sensor (Seapoint Chlorophyll Fluorometer; Seapoint Sensors, Inc.). Light penetration within the water column was calculated from vertical profiles using a PUV-542T spectral radiometer (Biospherical Instruments Inc., USA; later on abbreviated as PUV). The GUV and the PUV instruments were set to measure the irradiances of wavelengths both in the visible (PAR, in μE cm^{-2} s^{-1}) and in the ultraviolet range (305 and 313 nm for UVBR, and 320, 340 and 380 nm for UVAR, in μW cm^{-2}). The PUV profiler was cast in the water column before each sampling to determine sampling depths. The four sampling depths consisted of three depths in the euphotic zone (100, 50 and 0.1% of incident PAR) and one depth within the aphotic zone (Z_{aph}: 50 m below 1% of incident irradiance). During the last four sampling dates in spring, the second depth (50% of incident irradiance) was modified to sample the maximum of Chl-*a*. Moreover, when the difference between two preset depths was less than 10 m, only one sample was taken at an average in-between depth (see Fig. 2 for details of all

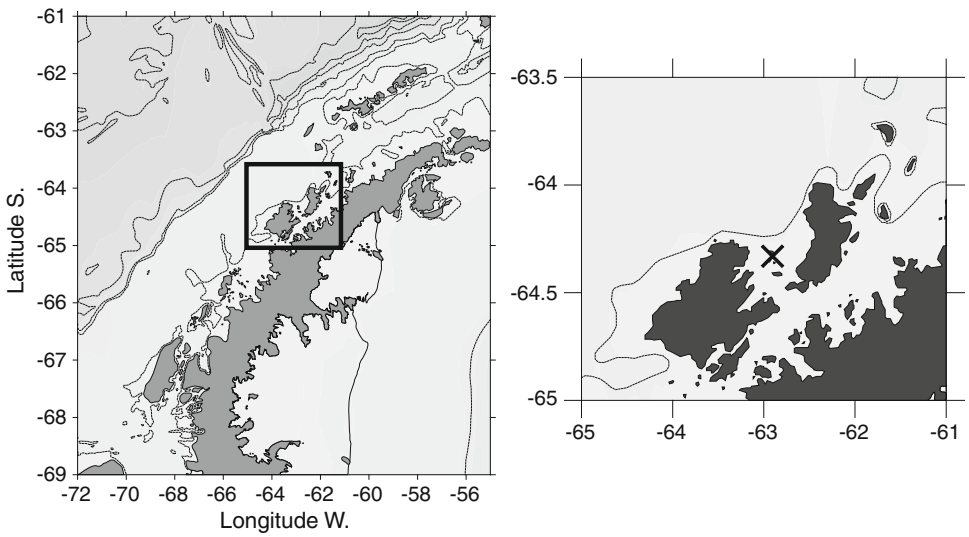

Fig. 1 The western Antarctic Peninsula (WAP) and the position of the sampling site north of Anvers Island (*cross*)

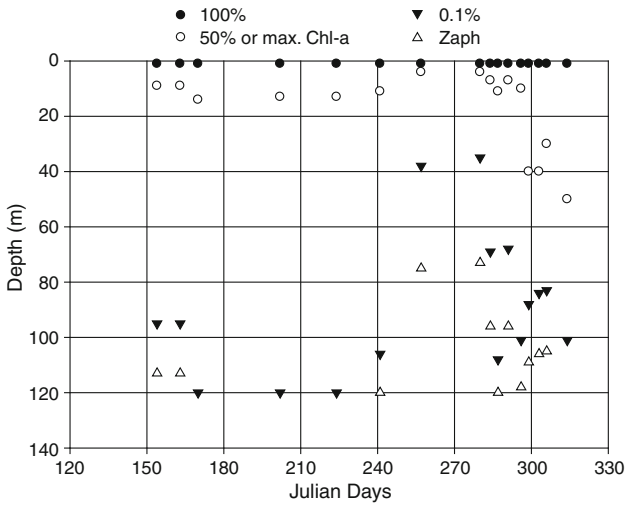

Fig. 2 Sampling depths for each day of sampling (given in Julian days). Depths corresponded to the penetration of light within the water column: 100%, 50% (or maximum of Chl-*a*) and 0.1% of incident irradiance and Z_{aph}

sampling depths). Water was then sampled using 5 l Niskin bottles.

Samples for the analysis of nutrients (nitrate, nitrite, phosphate and silicate) were filtered through precombusted Whatman GF/F filters, and filtrates were kept frozen (−20°C) until analysis. For phytoplankton pigment analysis, 950–1,000 ml of seawater was filtered on a 25-mm-diameter Whatman GF/F glass fiber filter. Filters were then wrapped in aluminum foil, immediately frozen in liquid nitrogen and stored at −80°C until analysis. Water aliquots for flow cytometric analyses of bacteria and picophytoplankton and nanophytoplankton were fixed with glutaraldehyde (final concentration 0.1%) into 4.5-ml cryovials in triplicate and stored at −80°C. Samples for phytoplankton (nanophytoplankton and microphytoplankton) and heterotrophic protist identification and enumeration were fixed in acid iodine Lugol solution at 2% final v/v concentrations and kept at 4°C in 300-ml glass amber bottles. Bacterial richness was estimated from two 500-ml aliquots of seawater filtered on white polycarbonate membrane (PC) of 25 mm diameter and 0.2 µm pore size (ISOPORE^{TM}), and filters were subsequently stored at −80°C in sterile Petri dishes. Bacterial richness was only analyzed at the two extreme depths (the surface and Z_{aph}).

Analysis of physical conditions

Daily stratospheric ozone concentration over the study site was obtained from http://toms.gsfc.nasa.gov/. The ozone hole was considered to be present over the study site when stratospheric ozone thickness was below 220 Dobson Units (DU) according to NASA's definition (http://ozonewatch.gsfc.nasa.gov/). Sea-ice concentration data were obtained from NASA's Nimbus-7 Scanning Multichannel Microwave Radiometer (SMMR) and Defense Meteorological Satellite Program (DMSP) -F13 Special Sensor Microwave/Imager (SSM/I). Daily sea-ice percent concentration for the year 2006 was obtained from the EOS Distributed Active Archive Center (DAAC) at the National Snow and Ice Data Center, University of Colorado in Boulder, Colorado (http://nsidc.org) (Cavalieri et al. 2008). Sea-ice concentration was defined as the percent cover of sea-ice on a 25 × 25 km square around the sampling site. For the purpose of this study, sea-ice retreat was defined as the last day of the year that sea-ice concentration was above 15% (Stammerjohn et al. 2008).

The fluorescence profiles were calibrated with extracted values of Chl-*a*, determined by HPLC (see below). For each sampling day, Chl-*a* concentrations were depth-integrated from the surface to the bottom of the euphotic layer,

and mean values were calculated by dividing the depth-integrated value by the integration depth (Heywood et al. 2006). The stability of the water column was estimated as in Sabatini et al. (2004) from the Simpson stability parameter (Simpson 1981), which is a measure of the mechanical work required to vertically mix the water column. A value >40 J m^{-3} for the Simpson parameter was considered to define a well-stratified water column (Sabatini et al. 2004). The depth of the upper mixed layer (Z_{UML}) was measured using the threshold gradient method described in Thomson and Fine (2003).

The attenuation coefficients, K_d, were calculated from the Beer–Lambert's law (Kirk 1983). The 10 and 1% penetration depths of incident light corresponding to each wavelength were calculated as: $Z_{10\%} = 2.3/K_d$ and $Z_{1\%} = 4.6051/K_d$ (Kirk 1983). The depth of the euphotic zone was defined as $Z_{1\%}$ (PAR) (Z_{eu}), and the photoactive depth of each UV radiation (UVR) wavelength ($Z_{ph}(\lambda)$; i.e. the depth at which the effects of UVBR and UVAR cease) as $Z_{10\%}$ (Neale et al. 2003). Because the water column was very clear during fall, winter and early spring (i.e. the sampling period), the attenuation of light within the water column did not show important variation. Therefore, the average $K_d(\lambda)$ is presented in Table 1 along with the depth penetration of each wavelength.

The penetration of UVR within the water column was difficult to determine during austral winter due to the very low light reaching the surface of the ocean and the PUV detection limits. Because the GUV recorded the incident irradiance above the water surface every day, it was possible to estimate the irradiance just below the water surface for every day of the sampling period from GUV records. To do so, the average K_d of each wavelength was considered and the transmission of light through the water surface was estimated. The penetration of light depends upon the illumination conditions (i.e. direct versus diffuse sky light) and the sea roughness (Arrigo 1994). While the transmittance of diffuse light is nearly constant, with an approximate value of 93.4% (Morel 1991), the transmittance of direct light strongly depends upon the solar zenith angle and the sea surface roughness (Haltrin et al. 2000). However, the GUV recorded the total incident irradiance and did not differentiate between direct and diffuse light. The large specular reflexion values at a high sun zenith angle (e.g. 60°), however, are compensated by the increasing proportion of the diffuse component of the total incident irradiance. Calculations show that the transmittance coefficients of total incident irradiance for a sun zenith angle >60° under a clear sky are, on average, about 84% in the visible (500 nm) and 93% in the UVBR (305 nm; S. Bélanger, personal communication). To simplify, a transmittance value of 90% was chosen to estimate the irradiance just below the water surface from GUV records for the whole sampling period. This method was tested by comparing the results with the actual measures of each wavelength obtained with the PUV when the water was sampled. The method proved to be a good approximation for each wavelength with all correlation coefficients between 0.8 and 0.85 ($P < 0.01$).

Because sea-ice cover is a major physical barrier, the penetration of light within the water column will be considered insignificant when sea-ice cover was above 15%. To determine the effect of UVBR on surface waters, each UVR wavelength was weighted for its potential impact on microorganisms DNA (Setlow 1974). Moreover, E_{ph}, the total irradiance integrated from the surface to the photoactive depth of each UVR wavelength (Z_{ph}), was calculated following the equation of Neale et al. (1991) that was slightly modified:

$$\int_0^{z_{ph}} E(\lambda).dz = \frac{E_{0-}(\lambda)}{K_d(\lambda)}\left(1 - e^{-K_d(\lambda).z_{ph}(\lambda)}\right)$$

with $E_{0-}(\lambda)$ the incident irradiance just below the water surface and $E_z(\lambda)$ the irradiance at depth z. Therefore, the potential impact of UVR on microorganisms' DNA could be estimated for the surface waters (i.e. to the depth of the photoactive zone). The results obtained were correlated with ozone concentration to determine the effect of the ozone hole in increasing UVBR transmission through the atmosphere. As expected, E_{ph} only correlated significantly with ozone thickness for UVBR wavelengths (i.e. with 313 nm, $r = -0.44$, $P < 0.01$). The penetration of 305 nm within the atmosphere is more sensitive to the concentration of stratospheric ozone than 313 nm. Therefore, one would expect E_{ph} (305 nm) to correlate with ozone concentration. However, because 305 nm is attenuated in the water column much faster than 313 nm and because the photoactive depth of 305 nm (7 m) is shallower than that of 313 nm (10 m), 313 nm was a better representative of the actual level of UVBR in the surface waters.

Table 1 Average $K_d(\lambda)$ (±SD) for UVBR, UVAR and PAR and corresponding depth ($m \pm$ SD) for the penetration of 10% of UVBR and UVAR (Z_{ph}) and of 1% of PAR (Z_{eu}) in the water column

	PAR	305 nm	313 nm	320 nm	340 nm	380 nm
$K_d(\lambda)$	0.06 ± 0.02	0.33 ± 0.03	0.24 ± 0.04	0.19 ± 0.03	0.15 ± 0.02	0.09 ± 0.01
Z_{ph} (UVBR & UVAR) and Z_{eu} (PAR) in meters	72 ± 24	7 ± 0.56	9.6 ± 1.46	12.4 ± 2.27	15.7 ± 1.74	25.4 ± 3.39

Sample analysis

Nutrient concentrations were determined using a Bran Luebbe AutoAnalyzer 3 system following Grasshof et al. (1983). Phytoplankton pigments were measured by high performance liquid chromatography (HPLC) using a Thermo Fisher system according to the method of Zapata et al. (2000). Pigments were detected using a photodiode-array spectrophotometric detector (UV-6000) in series with a FL 3000 fluorescence detector. Pigments were identified using their retention time, visible spectrum and comparison with standards from DHI Water and Environment (Hørsholm, Denmark).

Bacteria, picophytoplankton and nanophytoplankton were enumerated using an EPICS® ALTRA™ cell sorting flow cytometer (Beckman Coulter® Inc.) equipped with a laser emitting at 488 nm. Fluorescent beads (Fluoresbrite YG microspheres 1 and 1.9 µm for bacteria and phytoplankton, respectively, Polysciences™) were systematically added to each sample as an internal standard to normalize cell fluorescence emission and light scatter values. For the analysis of bacterial abundance, frozen samples were thawed, and two subsamples of 1 ml were half-diluted in TE 10× buffer (100 mM Tris–HCl, 10 mM EDTA, pH 8.0). One ml of the resulting diluted sample was stained with 0.3 µl of SYBR® Green I nucleic acid gel stain (Ci = 10,000×, Invitrogen, Inc), incubated for 10 min at room temperature in the dark (Lebaron et al. 2001) and analyzed for 240 s. For the analysis of phytoplankton abundance, frozen samples were thawed, and 1 ml of the sample was analyzed for 300 s. To calculate bacterial and phytoplankton cell abundances, the volume analyzed was calculated by weighing samples before and after each run. Total free bacteria (TB) were detected in a plot of green fluorescence recorded at 530 ± 30 nm (FL1) versus side angle light scatter (SSC). Bacteria with high and low nucleic acid content (HNA and LNA subgroups, respectively) were discriminated by gating the FL1-versus-SSC plot, and respective abundances of both subgroups were determined (Lebaron et al. 2001). For the purpose of this study, TB abundance was used to describe the bacterial community distribution, and %HNA (the ratio of HNA cells on TB) was used to describe the physiological structure of the bacterial community as suggested by different studies (Gasol et al. 1999; Gasol and Giorgio 2000; Lebaron et al. 2001; Vaqué et al. 2002). Picophytoplankton and nanophytoplankton were detected in a plot of red fluorescence recorded at 675 ± 5 nm (FL4) versus forward side scatter (FSC). Picophytoplankton was defined as phytoplankton smaller than 2 µm and nanophytoplankton as phytoplankton comprised between 2 and 20 µm. All cytometric analyses were performed under the Expo 32 v1.2b software (Beckman Coulter® Inc.). The size of organisms was determined through the construction of a calibration curve using 1, 2, 4, 5.9, 9.7 and 15.5 µm diameter large polystyrene microspheres (Molecular Probes Inc.). The carbon content of microorganisms, based on their abundance and size measured by flow cytometry, was calculated using different conversion factors for the different size classes: 220 fg C μm^{-3} for nanophytoplankton (Tarran et al. 2006), 1.5 pg C $cell^{-1}$ for picophytoplankton and 12 fg C $cell^{-1}$ for bacteria (Zubkov et al. 2000a, b).

Furthermore, nanophytoplankton, microphytoplankton and microzooplankton were identified and enumerated on Lugol-fixed samples using a Leitz Diavert inverted, phase-contrast microscope. Due to time constraints, only samples from the second depth, corresponding to the maximum of Chl-*a*, were analyzed. The biovolume (V) of cells was calculated using the geometric shapes proposed by Hillebrand et al. (1999) and corrected to account for cell shrinkage caused by fixation of samples (Montagnes et al. 1994). The carbon content of cells was calculated with two different carbon-to-volume ratios: pg C $cell^{-1} = 0.288\ V^{0.811}$ for diatoms and pg C $cell^{-1} = 0.216\ V^{0.939}$ for all other groups (Menden-Deuer and Lessard 2000).

Bacterial richness was analyzed at the two extreme depths (100% of incident irradiance and Z_{aph}). Total DNA extraction was performed using a classic Phenol–chloroform–isoamyl alcohol (25/24/1; 900 µl) protocol. PCR amplification of the 16S rDNA gene was then performed using a Mastercycler epS (Eppendorf) thermal cycler following the method proposed by Schäfer and Muyzer (2001). Three PCR amplifications were performed on each DNA sample to overcome the effect of PCR biases (Perreault et al. 2007). Amplicons were then purified with the MinElute (QIAGEN) columns according to the manufacturer's instructions and stored at −20°C until denaturing gradient gel electrophoresis (DGGE) analysis. DGGE was performed using a DGGE-4001-Rev-B (C.B.S. Scientific Company, CA, USA) system according to Schäfer and Muyzer (2001). Gels were then stained with a half-diluted solution of SYBR Green I (10,000×, Molecular Probes, Oregon) for 1 h according to the manufacturer's instructions. Gels were photographed under UV light, and DGGE profiles were analyzed using an AlphaImager® HP (Alpha-Innotech). The number of bands, corresponding to different operational taxonomic units (OTU), was determined visually for each sample. A similarity matrix using Jaccard's distance index was used to compare the fingerprints.

Statistical analyses

Seasons were defined according to the southern hemisphere winter solstice (June 21) as well as the spring equinox

(September 22). Statistical analyses were performed using the Statistica software (StatSoft® Inc). Normality was tested using Kolmogorov–Smirnov's and Shapiro–Wilk's tests, and homoscedasticity was verified using Levine's test. When normality and/or homoscedasticity were not met, data were transformed. Pearson (r) or Spearman rank (r_s) correlation coefficients were calculated to study the interdependence between abiotic (PAR, UVBR, UVAR, nutrient concentration, temperature, salinity, dissolved organic carbon concentration (DOC, data not shown) and particulate organic carbon and nitrogen concentrations (POC and PON, data not shown)) and biotic variables (TB, %HNA, pico-, nano-, microphytoplankton and microzooplankton abundances). The temperature and salinity of each sampling depth were obtained from the CTD profiles. The concentrations of DOC, POC and PON were obtained from Wang et al. (2009). Differences between depths were analyzed by t tests, whereas seasonal differences for biological and physical parameters were tested with ANOVAs.

To study the effects of stratospheric ozone loss and related UVBR increase on microorganisms in the field, the ratio between the abundance of organisms at the surface and at a sampling depth immediately below the UML was correlated with E_{ph} (313 nm), which best reflects the loss of stratospheric ozone and the increase in UVBR penetrating through the water column. These calculations were performed for bacterioplankton, %HNA, bacterial richness and for picophytoplankton and nanophytoplankton only because microphytoplankton and microzooplankton data only existed at the depth of 50% of incident irradiance. The rationale for the use of such biological ratios is that the changes in the relative abundance of microorganisms above and below the upper mixed layer would reflect significant effects of UVBR in surface waters (Helbling et al. 2005; Hernando and Ferreyra 2005). The ratios for picophytoplankton and nanophytoplankton were $\log_{10}$-transformed to meet the assumption of normality and homoscedasticity, while E_{ph} (313 nm) was arcsine (square root) transformed.

Results

Environmental conditions

In Fig. 3a, the irradiances at 305, 313 and 380 nm, estimated just under the water surface, are presented for the sampling period. An important daily variation in irradiance, related to cloud cover and albedo, can be observed for all wavelengths. As expected, an increase in UVAR (380 nm) was observed from winter to spring (i.e. a slope of 0.21 μW cm^{-2} day^{-1}). Although not presented in Fig. 3a, the same pattern was observed for both 320 and 340 nm. Shorter wavelengths such as 305 and 313 nm also increased regularly during spring time, but their rise was less pronounced and punctuated by episodes of significant elevation. Because 305 and 313 nm correlated negatively with ozone thickness ($r = -0.66$, $P < 0.01$ and $r = -0.47$, $P < 0.01$ for 305 and 313 nm, respectively), we can assess that these episodes of increased UVBR corresponded to both ozone loss periods and the onset of the spring season. Indeed, a significant decrease in ozone concentration (i.e. an ozone hole with ozone thickness <220 DU) was observed over the study site from the 31st of August to the 9th of October 2006 (day 243 to day 282 included; Fig. 3b). During this 40-day period, the minimum ozone thickness observed was 132 DU, and ozone thickness was below 220 DU on 33 occasions (averaging 192.9 ± 37 DU).

Sea-ice covered the sampling area during winter, except from the 10th to the 16th of September (day 253 to day 259 included) when it suddenly retreated (Fig. 3c). Ozone thickness was below 220 DU on 6 occasions during this transient retreat. Sea-ice then covered again the sampling area from the 17th of September to the 12th of October (day 260 to day 285 included), and therefore, sea-ice still covered the sampling area 4 days after the ozone hole disappeared. The water column was thus protected from increased UVBR by sea-ice cover during most of the ozone hole period. However, as seen in Fig. 3b, because of the onset of the spring season and because ozone recovery was not immediate after the ozone hole period, high intensities of UVBR penetrated the water column for the remaining of the sampling period. Indeed, high values of E_{ph} (313 nm) were encountered between the 13th of October and the 10th of November (day 286 to day 314, Fig. 3b). For example, during this period, the intensity at 320 nm just below the water surface varied from 4 to 17.8 μW cm^{-2} (with an average of 9.7 μW cm^{-2}). As a comparison, Helbling et al. (1995) found that only 3 and 0.1% of two bacterial strains (*Acinetobacter* sp. and *Bacillus* sp. respectively) could survive a radiation intensity of 9.6 μW cm^{-2} at 320 nm. In addition, Helbling et al. (1994) found that an intensity of 6 μW cm^{-2} at 320 nm at the surface could reduce primary production by 85%.

The Simpson parameter ranged between 21 and 32 J.m^{-3} during fall (average Z_{UML} of 35 m; Fig. 3d) and averaged 12.4 J m^{-3} during winter (average Z_{UML} of 48 m). During spring, the Simpson parameter increased regularly and was above 40 J m^{-3} after the 23rd of October (day 296). As a consequence, the UML became shallower in spring and was 22.6 m deep on average and as shallow as 16 m on day 296 (23rd of October). In addition, the photoactive depth, Z_{ph}, for UVBR laid from 10 to 12 m deep in spring, and the UML was therefore highly exposed to UVBR at this time of the year (Table 1).

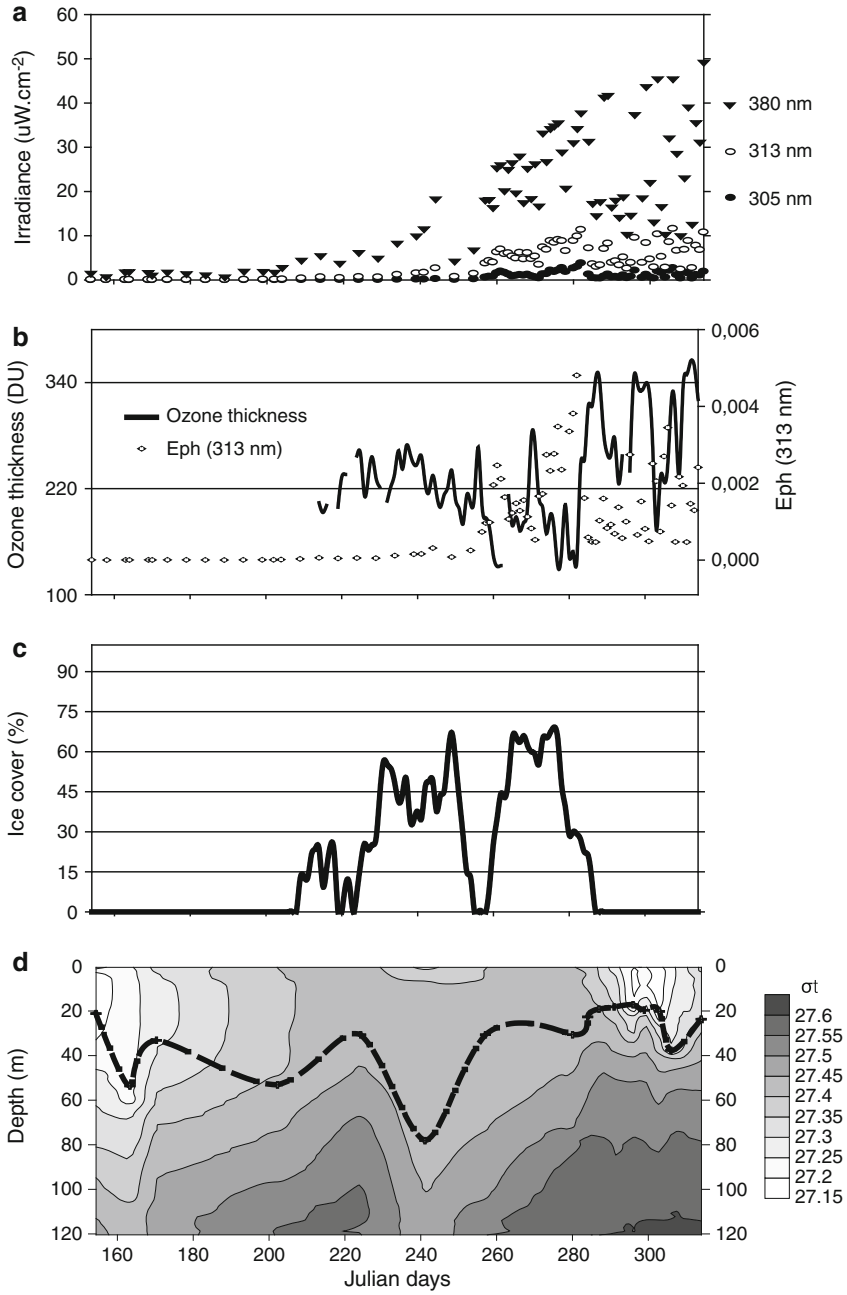

Fig. 3 **a** Incident irradiance at 305, 313 and 380 nm estimated below the water surface at local noon time (μW cm^{-2}); **b** Stratospheric ozone thickness (DU) and E_{ph} (313 nm); **c** Sea-ice concentration (%) and **d** Depth of the UML (m, *black dashed line*) and contour plot of σ_t for the sampling period

Surface water temperature was always below zero during the study. It decreased from fall (average of -0.78 ± 0.2°C) to winter (average of -1.62 ± 0.13°C), before increasing in spring (average of -1.04 ± 0.47°C). Surface water salinity followed an opposite pattern, increased from fall (average of 33.91 ± 0.05 PSU) to winter (average of 34.04 ± 0.04 PSU), before decreasing in spring (average of 33.94 ± 0.11 PSU). During this study, average concentrations of phosphate, nitrate and nitrite, and silicate through the water column were 2.3 ± 0.3, 27.7 ± 1.8 and 37 ± 8.5 μM, respectively. Across all depths, nutrient concentrations did not vary significantly ($P > 0.05$, Table 2) except at the surface in spring where nitrite and nitrate concentration decreased with a minimum observed concentration of 23.1 μM.

Bacterioplankton seasonal and vertical distributions and richness

During our survey, TB abundance ranged from 1.2×10^5 to 2.8×10^5 cells ml^{-1} (Fig. 4a; Table 3), decreased with depth ($r_s = -0.47$, $P < 0.01$), was significantly lower in

Table 2 Average nutrient concentration (μM ± SD) for each season (fall, winter and spring) and depth (100, 50 or 0.1% of incident irradiance and Z_{aph})

	Phosphate	Nitrite + Nitrate	Silicate
100%			
Fall	1.98 ± 0.04	25.83 ± 1.24	36.83 ± 15.45
Winter	2.02 ± 0.18	27.87 ± 0.58	34.97 ± 9.09
Spring	2.01 ± 0.08	25.04 ± 1.09	46.58 ± 11.99
50% or max. Chl-*a*			
Fall	2.05 ± 0.07	25.45 ± 0.35	47.93 ± 1.8
Winter	2.02 ± 0.79	27.84 ± 1.71	37.17 ± 4.31
Spring	2.39 ± 0.08	28.58 ± 0.72	34.50 ± 4.8
0.1%			
Fall	2.15 ± 0.28	28.05 ± 0.99	33.55 ± 1.84
Winter	2.11 ± 0.14	27.64 ± 0.34	30.3 ± 1.1
Spring	2.42 ± 0.14	29.73 ± 0.94	37.84 ± 6.83
Z_{aph}			
Fall	2.28 ± 0.11	28.58 ± 0.25	33.88 ± 1.38
Winter	1.94 ± 0.49	28.28 ± 0.88	32.79 ± 3
Spring	2.55 ± 0.2	27.98 ± 1.58	31.82 ± 3.17

winter ($P < 0.01$), more specifically for 100 and 50% of incident irradiance ($P < 0.01$ and $P < 0.05$, respectively), and increased from winter to spring. At the surface and 50% of incident irradiance, TB correlated positively with total phytoplankton abundance ($r = 0.64$ and $r = 0.73$, $P < 0.01$), nanophytoplankton abundance ($r = 0.55$, $P < 0.05$ and $r = 0.65$, $P < 0.01$) and water temperature ($r = 0.66$, $P < 0.05$ and $r = 0.64$, $P < 0.01$). In contrast, no significant seasonal variations in TB were observed at 0.1% of incident irradiance and Z_{aph}. In addition, the biomass of bacterioplankton at 50% of incident irradiance increased significantly ($P < 0.01$) from winter to spring (average of 2.8 ± 0.44 μg l^{-1}; Fig. 5a).

The bacterial community was constantly dominated by HNA (Table 3), and %HNA increased significantly with depth ($r_s = 0.32$, $P < 0.05$). No seasonal variations in %HNA were observed, and %HNA was not related to any biotic or abiotic variables. On the other hand, bacterial richness averaged 52.4 ± 6.9 OTUs per sample during the whole sampling period (Table 3). The Jaccard index showed a gradual decrease in bacterial richness in surface samples through the whole survey, while bacterial richness increased at Z_{aph} (Table 3). The decrease in bacterial richness at the surface was mainly attributable to the disappearance of non-dominant OTUs (represented by low intensity bands), while the contrary was true for Z_{aph}. Moreover, bacterial richness at the surface in spring was negatively correlated with E_{ph} (313 nm) ($r = -0.77$, $P < 0.01$), suggesting a possible cause for the decrease in bacterial richness at the surface in the spring.

Phytoplankton seasonal and vertical distribution and composition

Mean Chl-*a* integrated over the water column remained low during the whole period of study and never exceeded 0.3 μg l^{-1}, averaging 0.13 μg l^{-1} during fall and winter and 0.22 μg l^{-1} in spring (Fig. 4b). As shown in Fig. 4b, a sub-surface Chl-*a* maximum developed during spring time between ~30 and ~50 m deep (43 m on average), and the maximum estimated Chl-*a* concentration was 1.13 μg l^{-1}.

In terms of size classes, microphytoplankton was rare, and phytoplankton was always dominated numerically by picophytoplankton and nanophytoplankton from fall to spring. Microphytoplankton abundance at the depth of 50% irradiance averaged 1.38 ± 1.4 cells ml^{-1} throughout the sampling period (Table 3) and was higher in spring (average of 2.06 ± 1.69 cells ml^{-1}) than during either fall or winter (average of 0.45 ± 0.11 and 0.73 ± 0.47 cells ml^{-1}, respectively). Nanophytoplankton abundance ranged from 0.13 to 4.56 × 10^3 cells ml^{-1} and was significantly higher in spring than during either fall or winter ($P < 0.01$). More specifically, nanophytoplankton abundance increased significantly across seasons at the surface and 50% of incident irradiance ($P < 0.01$; Fig. 4c; Table 3). In addition, nanophytoplankton abundance showed a positive correlation with PAR ($r = 0.52$, $P < 0.05$) for the surface, suggesting that it responded to increasing light availability in spring. Picophytoplankton abundance ranged from 0.09 to 2.24 × 10^3 cells ml^{-1} and was more abundant at the surface and 50% of incident irradiance (ranging from 0.41 to 2.24 × 10^3 cells ml^{-1}) than at 0.1% of incident irradiance and Z_{aph} (ranging from 0.09 to 1.44 × 10^3 cells ml^{-1}, Fig. 4d; Table 3). In contrast to nanophytoplankton, picophytoplankton average abundance (0.81 ± 0.44 × 10^3 cells ml^{-1}) did not vary significantly across seasons ($P > 0.05$), except at the surface where it decreased in spring ($P < 0.01$). It also appears that the ratios of nanophytoplankton and picophytoplankton abundance at the surface and below the pycnocline ($Nano_{surf}/Nano_{depth}$ and $Pico_{surf}/Pico_{depth}$) both showed negative correlation with E_{ph} (313 nm), although it was only significant for picophytoplankton ($r = -0.51$, $P > 0.05$ and $r = -0.77$, $P < 0.01$, for nanophytoplankton and picophytoplankton, respectively). This may suggest that UVBR had a negative impact on phytoplankton and more particularly on picophytoplankton.

In terms of community composition, dominant groups included pico-sized and nano-sized prymnesiophytes and autotrophic flagellates (respectively, averaging 39 ± 8.5% and 42.7 ± 7.8% of the phytoplankton abundance). Phytoplankton was further composed of nano-sized dinoflagellates such as *Gymnodinium* spp. and *Gyrodinium* spp. during winter (11.3 ± 4% of phytoplankton abundance)

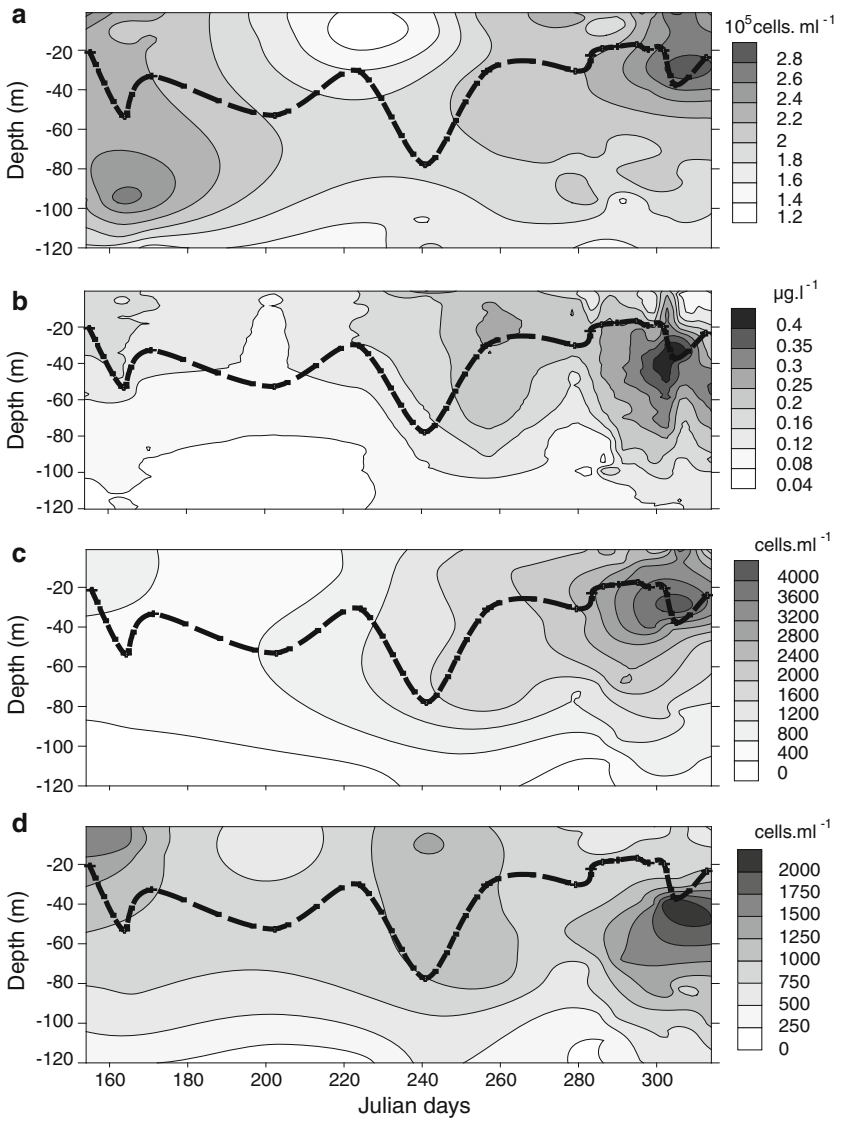

Fig. 4 Contour plots of **a** bacterial abundance (10^5 cells ml^{-1}); **b** Chl-*a* concentration (µg l^{-1}); **c** nanophytoplankton abundance (cells ml^{-1}) and **d** picophytoplankton abundance (cells ml^{-1}) for the sampling period. On each graph, the depth of the UML is indicated by a *black line*

and of nano-sized cryptophytes and pennate diatoms (respectively, 7.6 ± 7.9% and 3.3 ± 1.5% of phytoplankton abundance) and micro-sized centric diatoms such as *Chaetoceros aff. tenuissimus* and *Corethron hystrix* (1.4 ± 1% of phytoplankton abundance) during spring.

The carbon biomass of phytoplankton increased from fall and winter (7.2 ± 2.3 and 8.8 ± 4.1 µg C l^{-1}, respectively) to spring (25.5 ± 9.4 µg C l^{-1}; Fig. 5b). At the same time, the mean Chl-*a* at the depth of 50% of incident irradiance decreased from fall (0.21 µg l^{-1} in average) to winter (0.12 µg l^{-1} in average) before increasing again in spring (0.41 µg l^{-1} in average). Although prymnesiophytes and autotrophic flagellates dominated the phytoplankton in terms of abundance, they never contributed significantly to the total autotrophic carbon biomass but on one occasion during spring time (26th of October or day 299) when prymnesiophytes accounted for 49% of the phytoplankton carbon biomass. In agreement with microscopic data, an increase in pigments found in prymnesiophytes, such as Chl c_3 and 19′-hexanoyloxyfucoxanthin, was noticed on day 299 (data from M. Lionard and S. Roy, not shown). During fall and winter, nano-sized dinoflagellates accounted for most of the autotrophic carbon biomass (averaging 51.3 ± 20.4%). The typical dinoflagellate marker peridinin was not detected, but other pigments (Chl c_2, Chl c_3, 19′-hexanoyloxyfucoxanthin, fucoxanthin and diadinoxanthin) were present and could indicate the presence of dinoflagellates with acyl-fucoxanthin instead of peridinin. During spring time, the phytoplankton carbon biomass was dominated by micro-sized centric and pennate diatoms (29.6 ± 15.2% and 11.7 ± 10.3%, respectively) and by nano-sized dinoflagellates (25.6 ± 15% in average).

Table 3 Seasonal average (fall, winter and spring) of the abundance of total bacteria (TB, 10^5 cells ml^{-1}), %HNA, bacterial richness (OTUs), picophytoplankton (Pico, cells ml^{-1}), nanophytoplankton (Nano, cells ml^{-1}), microphytoplankton (Microphyto, cells ml^{-1}) and microzooplankton (Microzoo, cells ml^{-1}) at the depth of 100, 50 and 0.1% of incident irradiance and at Z_{aph}. Bacterial richness was only determined at 100% and Z_{aph}. Microphytoplankton and microzooplankton were only enumerated at the depth of 50% of incident irradiance

Depth	Season	TB	%HNA	Richness	Pico	Nano	Microphyto	Microzoo
100%	Fall	2.43 ± 0.22	58.2 ± 1.8	52.67 ± 1.16	1,373 ± 305	1,063 ± 120	ND	ND
	Winter	1.66 ± 0.33	66 ± 4	55.75 ± 1.5	876 ± 264	1,194 ± 498	ND	ND
	Spring	2.35 ± 0.30	64.4 ± 4	50.11 ± 6.11	557 ± 113	2,456 ± 716	ND	ND
50% or max Chl-*a*	Fall	2.24 ± 0.17	58.6 ± 0.6	ND	1,354 ± 311	1,071 ± 102	0.45 ± 0.11	50.3 ± 15.4
	Winter	1.64 ± 0.37	65.6 ± 5.8	ND	905 ± 298	1,316 ± 654	0.73 ± 0.47	51.5 ± 18.4
	Spring	2.29 ± 0.36	65.4 ± 3.1	ND	1,056 ± 638	2,920 ± 920	2.06 ± 1.69	108 ± 52.6
0.1%	Fall	2.14 ± 0.62	70 ± 7.1	ND	492 ± 236	317 ± 115	ND	ND
	Winter	1.69 ± 0.32	69.6 ± 3.6	ND	464 ± 427	697 ± 756	ND	ND
	Spring	1.96 ± 0.17	66.5 ± 2.8	ND	920 ± 369	1,480 ± 696	ND	ND
Z_{aph}	Fall	1.83 ± 0.30	59 ± 5.2	44.33 ± 4.16	339 ± 86	240 ± 55	ND	ND
	Winter	1.71 ± 0.24	70.5 ± 3.7	48 ± 8.37	481 ± 486	754 ± 924	ND	ND
	Spring	1.77 ± 0.19	68.1 ± 3	57.78 ± 5.95	617 ± 239	898 ± 305	ND	ND

ND not determined

Microzooplankton seasonal distribution and composition

Microzooplankton was composed of small heterotrophic flagellates (diameter range 3–10 μm), choanoflagellates (diameter range 10–20 μm), a 10-μm-diameter phagotrophic flagellate, *Telonema* sp. and ciliates dominated by *Strombidium aff. striatum* (30 μm diameter) and oligotrichous ciliates (diameter range 10–50 μm). Average microzooplankton abundance increased from fall and winter (50.3 ± 15.4 and 51.5 ± 18.4 cells ml^{-1}, respectively) to spring (108 ± 52.6 cells ml^{-1}, Table 3).

The abundance of small heterotrophic flagellates averaged 37.9, 38.4 and 71 cells ml^{-1} for fall, winter and spring, respectively. This represented 68 ± 14.4% of all microzooplankton for the whole sampling period, and small heterotrophic flagellates always dominated microzooplankton in terms of abundance. In contrast, they only accounted for a small part of the microzooplankton carbon biomass (0.82 ± 0.49 μg C l^{-1} or 17.1 ± 7.4% of the microzooplankton biomass). Ciliates' abundance and biomass were always low throughout the sampling period (0.5 ± 0.4 cells ml^{-1} and 0.25 ± 0.2 μg C l^{-1}), accounting for only 0.9 ± 0.9% and 6.4 ± 6.3% of the microzooplankton abundance and biomass, respectively. During fall and winter, choanoflagellates composed the remaining of the microzooplankton averaging 7.1 ± 4.2 cells ml^{-1} and 2.5 ± 1.5 μg C l^{-1}. This represented 13.8 ± 7.4% and 63 ± 25.4% of the microzooplankton abundance and biomass, respectively. A shift in the composition of microzooplankton occurred at spring time when *Telonema* sp. abundance and biomass increased (35 ± 14 cells ml^{-1} and 3.8 ± 1.6 μg C l^{-1}). This represented 35.3 ± 15.5% and 65 ± 17.3% of the microzooplankton abundance and biomass, respectively.

As shown in Fig. 5a, microzooplankton biomass at 50% of incident irradiance did not change from fall (average of 3.6 ± 0.9 μg l^{-1}) to winter (average of 3.7 ± 0.16 μg l^{-1}) but increased in spring (average of 5.7 ± 1.3 μg l^{-1}), although this difference was not significant ($P > 0.05$). In addition, microzooplankton biomass was positively correlated with phytoplankton and bacterioplankton biomass ($r = 0.73$ and $r = 0.71$ for phytoplankton and bacterioplankton, respectively, $P < 0.01$).

Discussion

Fall and winter conditions

As expected at this high latitude (Pearce et al. 2007), light was nearly absent in the study area during fall and winter while water temperature was below zero, creating inhospitable conditions for marine organisms. Despite nutrient availability, mean integrated Chl-*a* was low in fall and winter (averaging 0.3 and 0.13 μg l^{-1}, respectively) due to the absence of light and very low water temperature (below 0°C). During this low production period, bacterioplankton and microzooplankton biomass was also low compared to more productive times of the year. Finally, small cells (i.e. pico-sized and nano-sized) composed most of the autotrophic and heterotrophic biomass, suggesting the predominance of a microbial food web ecosystem (Legendre and Rassoulzadegan 1996).

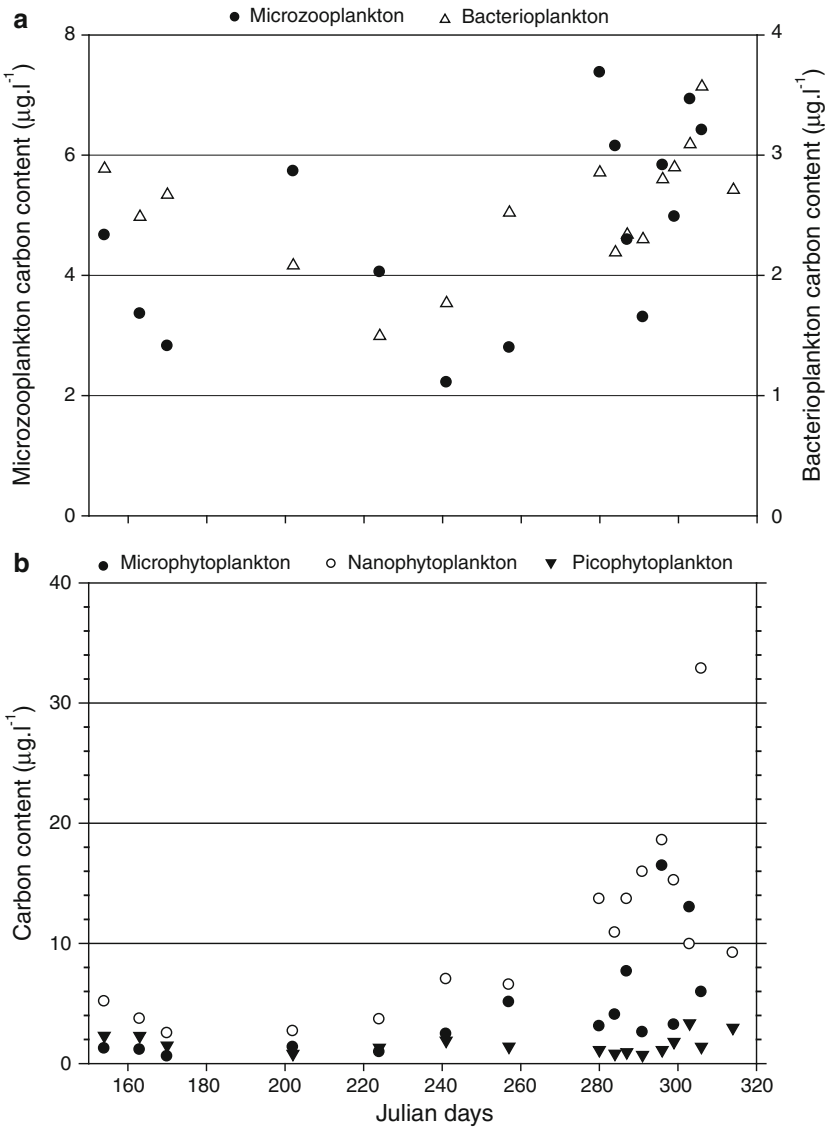

Fig. 5 Carbon content at the depth of 50% of incident irradiance of **a** microzooplankton and bacterioplankton (µg l^{-1}) and **b** picophytoplankton, nanophytoplankton and microphytoplankton (µg l^{-1})

The Southern Ocean, and hence the WAP waters, have been hypothesized to be rectified (one-way) annual CO_2 sinks, mainly because sea-ice is present during the less productive period of the year, while in the summer, when sea-ice is absent, production is maximum (Takahashi et al. 2002; Ducklow et al. 2007). Because of regional warming, Stammerjohn et al. (2008) have observed a decreasing winter sea-ice concentration in the WAP along with a later advance and an earlier retreat over the last decade. Therefore, there is now some doubt regarding the rectified sink hypothesis for WAP waters (Metzl 2009; Takahashi et al. 2009). In fact, sea-ice concentration was particularly low during the 2006 winter compared to the monthly average sea-ice concentrations for the last decade (Moreau et al. unpublished data). Indeed, in 2006, July and August average sea-ice concentrations were, respectively, 8 and 17% below the monthly average sea-ice concentration from 1998 to 2007. If, in the future, sea-ice is absent during the less productive seasons, the WAP waters may no longer be a rectified CO_2 sink.

Not surprisingly, Wang et al. (2009) determined that our study site acted as a CO_2 source during winter. Because water temperature ranges are very small in Antarctic waters, CO_2 fluxes in Antarctica are mainly driven by biological uptake and respiration (Takahashi et al. 2002). Moreover, the presence of a microbial food web leads the ocean to act as a source of CO_2 to the atmosphere (Schloss et al. 2007). We found that a microbial food web dominated at our study site during fall and winter. Therefore, the potential absence of a sea-ice cover during winter in the WAP may be a concern. Future information on microorganisms' composition and dynamics during winter will be important to determine carbon fluxes in Antarctica.

Spring: the onset of the production season

The average day of sea-ice retreat in this region for the last decade (1998–2007) was day 318 (Moreau et al., unpublished data). In 2006, sea-ice retreated on day 285 and therefore 33 days before the average retreat of sea-ice for the last decade. The disappearing of sea-ice corresponded to an increase in incident irradiance and water temperature along with high nutrient concentrations, creating suitable growth conditions for phytoplankton and the microbial community. An increase in phytoplankton abundance and biomass was indeed observed in spring, immediately following the retreat of sea-ice. This rise was slight, reaching a maximum Chl-*a* concentration of 1.13 μg l^{-1}, representative of what Morán et al. (2006) reported as the initial phase of the bloom period in the WAP. Morán et al. (2006) also associated temporary increase in particulate extracellular release (PER) with changes in the community composition toward the dominance of larger cells. This is in agreement with Wang et al. (2009) who observed a clear DOC increase in spring during our study, and with our observation that, during this phase, the community composition changed and most of the autotrophic biomass consisted of nano-sized cells. Therefore, the community started to resemble the richer herbivorous food web usually found in WAP waters in the late spring–summer season (e.g. Villafañe et al. 1993; Moline and Prézelin 1996; Garibotti et al. 2003).

Even though we observed some degree of phytoplankton biomass accumulation in spring following the immediate retreat of sea-ice, this accumulation was not as important as sometimes witnessed in the coastal WAP (e.g. in November 2002; Smith et al. 2008). In fact, from data collected near Palmer station, less than 80 km away from where this study was performed, this initial phase of the bloom lasted until mid to late-December when a significant spring bloom truly started (reaching up to 20.5 μg l^{-1} on the 26th of December 2006; M. Vernet, personal communication). Several factors may have prevented or delayed the phytoplankton bloom in November 2006. Of these factors, iron is not a limiting factor in Antarctic coastal waters (Martin et al. 1990) and probably did not limit phytoplankton biomass accumulation during our study. Compared to other studies (e.g. Holm-Hansen et al. 1994), phosphate, nitrate + nitrite, and silicate were in excess to support high levels of primary productivity and never became limiting throughout the study either. According to Mitchell and Holm-Hansen (1991), the depth of the UML and of the euphotic zone is critical in determining phytoplankton growth in the WAP waters. During this study, the UML was shallow in spring after sea-ice had retreated (22.6 m deep on average and as shallow as 16 m on day 296, 23rd of October), and Z_{eu} was deep (average of 72 m). Therefore, oceanographic conditions seemed to be adequate for growth.

Microzooplankton grazing may have delayed or prevented the expected phytoplankton bloom since it can be important in Antarctic waters (Pearce et al. 2008). Indeed, microzooplankton biomass was positively correlated with phytoplankton biomass, and, as suggested by Buck and Garrison (1988), this may imply that grazing controlled the phytoplankton community. Choanoflagellates largely dominated the microzooplankton biomass during fall and winter. Choanoflagellates are commonly found in Antarctica where they prey on bacteria and picophytoplankton (Buck and Garrison 1988), both of which were numerically dominant during fall and winter. At the beginning of spring, the composition of microzooplankton shifted, and *Telonema* sp. dominated the microzooplankton biomass. Phagotrophic flagellates such as *Telonema* sp. are known to prey on larger cells such as nanophytoplankton (Brandt and Sleigh 2000), which dominated the phytoplankton community in spring. Therefore, microzooplankton may have controlled phytoplankton to some extent. Moreover, such a switch in the type and size of microzooplankton from winter to spring has already been observed in Antarctica by Pearce et al. (2008) who found that microzooplankton was mainly composed of bacterivores during winter and herbivores during more productive periods (i.e. spring and summer).

Despite these apparently optimal growth conditions in spring, we observed only a small increase in bacterial abundance and no significant shift in the bacterial physiological structure (based on the %HNA). The factors that usually control bacterioplankton distribution, and that could have prevented a bacterioplankton bloom during this study, include resource limitation (Morán et al. 2002), grazing (Buck and Garrison 1988), viral lysis (Pearce et al. 2007) or other deleterious factors such as UVBR penetrating the water column (Buma et al. 2001). Phytoplankton is an important source of nutrients for bacterioplankton (Morán et al. 2006). In our study, we observed that bacterial abundance in the euphotic zone was positively correlated with phytoplankton abundance and more particularly with nanophytoplankton. Moreover, because of the low bacterial biomass encountered in this study, we believe that phytoplankton production met bacterial carbon demand in the investigated area and that bacterioplankton was not resource limited. In fact, a lag of approximately 1 month between the accumulation of new production in spring and the increase in bacterial abundance has previously been observed in Antarctic waters (Pearce et al. 2007, 2008). It is possible that the same lag was present here, but sampling stopped too early to detect the subsequent bacterial increase. On the other hand, microzooplankton biomass was positively correlated with bacterial

biomass, and, as suggested by Buck and Garrison (1988), this may imply that grazing had a major influence on the bacterial community.

Spring-time ozone hole and UVBR effects on surface waters

Ozone concentration in August 2006 was 9 DU lower than the average August ozone concentration from 1998 to 2007. The average ozone concentrations in September and October 2006 were very low (202 and 244 DU, respectively) and were consistent with the average ozone concentration observed from 1998 to 2007 (Moreau et al., unpublished data). Finally, 2006 is the year when the ozone hole attained its maximum area coverage (http://ozonewatch.gsfc.nasa.gov/). During our survey, sea-ice cover still protected the water column from increased UVBR 4 days after the ozone hole period (13th of October or day 285, Fig. 3c). However, ozone recovery was not immediate after day 285, and "low" ozone thickness episodes (average of 293.8 ± 51.3 DU) were observed during ozone recovery (mid-October to December, Fig. 3b). As a consequence, high-intensity UVBR reached the surface of the water column after the ozone hole period and for the remaining of the sampling period (from the 13th of October to the 10th of November, Fig. 3b). Indeed, the intensities of UVBR measured under the water surface during this study are comparable to other studies that reported strong inhibition of primary production (Helbling et al. 1994) or mass mortality of bacterioplankton (Helbling et al. 1995).

Bacterial richness was negatively correlated with E_{ph} (313 nm) during our study, suggesting negative effects of UVBR. In fact, bacterial richness decreased at the surface in spring, which is in accordance with the findings of Murray et al. (1998). These authors believed that other factors such as water column stability, depth or season could be responsible for the decrease in bacterial richness observed in spring. Considering our data, it seems that UVBR might also influence bacterial richness in surface waters in spring, possibly by selecting for UVBR-resistant species. However, this result needs further studies to be confirmed. Moreover, the ratios $Nano_{surf}/Nano_{depth}$ and $Pico_{surf}/Pico_{depth}$ were both inversely correlated with E_{ph} (313 nm) (although it was only significant for picophytoplankton). This suggests that UVBR had negative effects on phytoplankton in surface waters (for a review of potential effects see Häder and Sinha 2005).

UVBR are deleterious for marine organisms, and photorepair processes are more efficient in deeper waters where low values of the UVBR:UVAR ratio are encountered (Kaiser and Herndl 1997). Moreover, the degree and extent of exposure to UVBR are important in determining the impact these radiations can have (Helbling et al. 1996; Davidson and Belbin 2002). Therefore, water column stratification will be a major factor determining how these radiations affect the microbial community (Xenopoulos et al. 2000; Hernando and Ferreyra 2005). When increased UVBR reached the water column of the WAP in spring, the upper mixed layer was as shallow as 16 m and the photoactive depth for UVBR was relatively deep (10–12 m). Therefore, the upper mixed layer was highly exposed to UVBR. Under these conditions, microorganisms were confined within a shallow UML and were probably undergoing significant stress from UVBR (Häder and Sinha 2005; Hernando et al. 2005). DNA photorepair was probably less efficient, and microorganisms would have accumulated DNA damage (i.e. cyclobutane pyrimidine dimers or CPDs; one of the major DNA lesion caused by UVR) (Häder and Sinha 2005). Moreover, as described by Helbling et al. (2005), photoinhibition was probably strong in surface waters. Therefore, we hypothesize that UVBR had an impact on surface water microorganisms early in spring, when no ice cover could shield the water column.

Conclusions

In conclusion, the abundance and biomass of the microbial community (bacterioplankton, phytoplankton and microzooplankton) were low in fall and winter 2006 at our study site, and the microbial community was dominated by small cells (pico-sized). Following the retreat of sea-ice, an increase in bacterial and phytoplankton abundance and biomass was observed in spring. However, despite seemingly optimal growth conditions, this increase was small. Microzooplankton grazing may have prevented or delayed the typical WAP bloom. In addition, the early disappearing of sea-ice in spring 2006 let the water column exposed to increased UVBR, which seemed to have had an impact on bacterial richness and on phytoplankton abundance and composition in surface waters. This study suggests that the dynamics of the microbial community in the WAP at this time of the year can be controlled by the interaction of several biological and physical factors. In the context of global warming, decreasing sea-ice season and delayed stratospheric ozone recovery for the next decades, more studies of the WAP microbial food web functioning during winter and early spring should be encouraged.

Acknowledgments This research was funded by the NSERC Special Research Opportunity Program grant nr. 334876-2005 conceded to Serge Demers. Daily stratospheric ozone concentrations over the study site were obtained from http://toms.gsfc.nasa.gov/. The 2006 SMMR-SSM/I sea-ice concentration data were obtained from the EOS Distributed Active Archive Center (DAAC) at the National Snow and Ice Data Center, University of Colorado in Boulder, Colorado (http://nsidc.org). We would like to thank Sylvie Lessard for

her help in identifying microorganisms under an inverted microscope. We would also like to thank Damian López, as well as the Sedna IV crew and his leader Jean Lemire, for their strong support during the field sampling in Antarctica.

References

Arrigo KR (1994) Impact of ozone depletion on phytoplankton growth in the Southern Ocean: large-scale spatial and temporal variability. Mar Ecol Prog Ser 114:1–12. doi:10.3354/meps114001

Arrigo KR, Thomas DN (2004) Large scale importance of sea ice biology in the Southern Ocean. Antarct Sci 16:471–486. doi:10.1017/S0954102004002263

Arrigo KR, Dijken GV, Pabi S (2008) Impact of a shrinking Arctic ice cover on marine primary production. Geophys Res Lett 35:1–6. doi:10.1029/2008GL035028

Bouchard JN, Roy S, Campbell DA (2006) UVB effects on the Photosystem II-D1 protein of phytoplankton and natural phytoplankton communities. Photochem Photobiol 82:936–951. doi:10.1562/2005-08-31-IR-666

Brandt SM, Sleigh MA (2000) The quantitative occurrence of different taxa of heterotrophic flagellates in Southampton water. UK Estuar Coast Shelf Sci 51:91–102. doi:10.1006/ecss.2000.0607

Brightman RI, Smith WO Jr (1989) Photosynthesis-irradiance relationships of Antarctic phytoplankton during austral winter. Mar Ecol Prog Ser 53:143–151

Buck KR, Garrison DL (1988) Distribution and abundance of choanoflagellates (Acanthoecidae) across the ice-edge zone in the Weddell Sea, Antarctica. Mar Biol 98:263–269. doi:10.1007/BF00391204

Buma AGJ, de Boer MK, Boelen P (2001) Depth distributions of DNA damage in Antarctic marine phyto- and bacterioplankton exposed to summertime UV radiation. J Phycol 37:200–208. doi:10.1046/j.1529-8817.2001.037002200.x

Cavalieri D, Parkinson C, Gloersen P, Zwally HJ (2008) Sea ice concentrations from Nimbus-7 SMMR and DMSP SSM/I passive microwave data, [2006]. National Snow and Ice Data Center. USA Digital media, Boulder

Church MJ, DeLong EF, Ducklow HW, Karner MB, Preston CM, Karl DM (2003) Abundance and distribution of planktonic Archaea and Bacteria in the waters west of the Antarctic Peninsula. Limnol Oceanogr 48:1893–1902

Cockell CS, Córdoba-Jabonero C (2004) Coupling of climate change and biotic UV exposure through changing snow–ice covers in terrestrial habitats. Photochem Photobiol 79:26–31. doi:10.1562/0031-8655(2004)79<26:COCCAB>2.0.CO;2

Cullen JJ, Neale PJ, Lesser MP (1992) Biological weighting function for the inhibition of phytoplankton photosynthesis by ultraviolet radiation. Science 258:646–650

Davidson A, Belbin L (2002) Exposure of natural Antarctic marine microbial assemblages to ambient UV radiation: effects on the marine microbial community. Aquat Microb Ecol 27:159–174. doi:10.3354/ame027159

Delille D (2004) Abundance and function of bacteria in the Southern Ocean. Cell Mol Biol 50:543–551

Ducklow HW, Baker K, Martinson DG, Quetin LB, Ross RM, Smith RC, Stammerjohn SE, Vernet M, Fraser W (2007) Marine pelagic ecosystems: the West Antarctic Peninsula. Philos Trans Royal Soc London B Biol Sci 362:67–94

Ferreyra GA, Mostajir B, Schloss IR, Chatila K, Ferrario ME, Sargian P, Roy S, Prod'homme J, Demers S (2006) Ultraviolet-B radiation effects on the structure and function of lower trophic levels of the marine planktonic food web. Photochem Photobiol 82:887–897. doi:10.1562/2006-02-23-RA-810

Frederick JE, Lubin D (1994) Solar ultraviolet radiation at Palmer Station, Antarctica. In: Weiler CS, Penhale PA (eds) Ultraviolet radiation in Antarctica: measurements and biological effects, Antartic research series, vol 62. American Geophysical Union, Washington, DC, pp 43–52

Garibotti IA, Vernet M, Ferrario ME, Smith RC, Ross RM, Quetin LB (2003) Phytoplankton spatial distribution patterns along the western Antarctic Peninsula (Southern Ocean). Mar Ecol Prog Ser 261:21–39. doi:10.3354/meps261021

Gasol JM, Giorgio PAD (2000) Using flow cytometry for counting natural planktonic bacteria and understanding the structure of planktonic bacterial communities. Sci Mar (Barc) 64:197–224. doi:10.3989/scimar.2000.64n2197

Gasol JM, Zweifel UL, Peters F, Fuhrman JA, Hagström Å (1999) Significance of size and nucleic acid content heterogeneity as measured by flow cytometry in natural planktonic bacteria. Appl Environ Microbiol 65:4475–4483

Grasshof K, Ehrahrdt M, Kremling K (1983) Methods of seawater analysis. Verlag Chemie, Weinheim

Häder DP, Sinha RP (2005) Solar ultraviolet radiation-induced DNA damage in aquatic organisms: potential environmental impact. Mutat Res-Fundam Mol Mech Mutag 571:221–233. doi:10.1016/j.mrfmmm.2004.11.017

Häder DP, Kumar HD, Smith RC, Worrest RC (2007) Effects of solar UV radiation on aquatic ecosystems and interactions with climate change. Photochem Photobiol Sci 6:267–285. doi:10.1039/b700020k

Haltrin VI, McBride Iii WE, Weidemann AD (2000) Fresnel reflection by wavy sea surface. International geoscience and remote sensing symposium (IGARSS). IEEE, Honolulu, HI, USA

Helbling EW, Villafane VE, Holm-Hansen O (1994) In situ inhibition of primary production due to ultraviolet radiation in Antarctica. Antarct J US 29:262–263

Helbling EW, Marguet ER, Villafane VE, Holm-Hansen O (1995) Bacterioplankton viability in Antarctic waters as affected by solar ultraviolet radiation. Mar Ecol Prog Ser 126:293–298. doi:10.3354/meps126293

Helbling EW, Chalker BE, Dunlap WC, Holm-Hansena O, Villafañe VE (1996) Photoacclimation of antarctic marine diatoms to solar ultraviolet radiation. J Exp Mar Biol Ecol 204:85–101. doi:10.1016/0022-0981(96)02591-9

Helbling EW, Barbieri ES, Marcoval MA, Gonçalves RJ, Villafañe VE (2005) Impact of solar ultraviolet radiation on marine phytoplankton of Patagonia, Argentina. Photochem Photobiol 81:807–818. doi:10.1562/2005-03-02-RA-452R.1

Hernando MP, Ferreyra GA (2005) The effects of UV radiation on photosynthesis in an Antarctic diatom (*Thalassiosira* sp.): does vertical mixing matter? J Exp Mar Biol Ecol 325:35–45. doi:10.1016/j.jembe.2005.04.021

Hernando MP, Malanga GF, Ferreyra GA (2005) Oxidative stress and antioxidant defences generated by solar UV in a Subantarctic marine phytoflagellate. Sci Mar (Barc) 69:287–295. doi:10.3989/scimar.2005.69s2287

Heywood JL, Zubkov MV, Tarran GA, Fuchs BM, Holligan PM (2006) Prokaryoplankton standing stocks in oligotrophic gyre and equatorial provinces of the Atlantic Ocean: evaluation of inter-annual variability. Deep Sea Res (II Top Stud Oceanogr) 53:1530–1547. doi:10.1016/j.dsr2.2006.05.005

Hillebrand H, Dürselen C-D, Kirschtel D, Pollingher U, Zohary T (1999) Biovolume calculation for pelagic and benthic microalgae. J Phycol 35:403–424. doi:10.1046/j.1529-8817.1999.3520403.x

Holm-Hansen O, Amos AF, Silva N, Villafañe V, Helbling EW (1994) In situ evidence for a nutrient limitation of phytoplankton

growth in pelagic Antarctic waters. Antarct Sci 6:315–324. doi:10.1017/S0954102094000489
Kaiser E, Herndl GJ (1997) Rapid recovery of marine bacterioplankton activity after inhibition by UV radiation in coastal waters. Appl Environ Microbiol 63:4026–4031
Kirk JTO (1983) Light and photosynthesis in aquatic systems. Cambridge University Press, Cambridge
Lawson GL, Wiebe PH, Ashjian CJ, Gallager SM, Davis CS, Warren JD (2004) Acoustically-inferred zooplankton distribution in relation to hydrography west of the Antarctic Peninsula. Deep Sea Res (II Top Stud Oceanogr) 51:2041–2072. doi:10.1016/j.dsr2.2004.07.022
Lebaron P, Servais P, Agogue H, Courties C, Joux F (2001) Does the high nucleic acid content of individual bacterial cells allow us to discriminate between active cells and inactive cells in aquatic systems? Appl Environ Microbiol 67:1775–1782
Legendre L, Rassoulzadegan F (1996) Food-web mediated export of biogenic carbon in oceans: hydrodynamical control. Mar Ecol Prog Ser 145:179–193. doi:10.3354/meps145179
Lesser MP, Lamare D, Barker MF (2004) Transmission of ultraviolet radiation through the Antarctic annual sea ice and its biological effects on sea urchin embryos. Limnol Oceanogr 49:1957–1963
Loeb V, Siegel V, Holm-Hansen O, Hewitt R, Fraserk W, Trivelpiecek W, Trivelpiecek S (1997) Effects of sea-ice extent and krill or salp dominance on the Antarctic food web. Nature 387:897–900
Marshall GJ, Lagun V, Lachlan-Cope TA (2002) Changes in Antarctic Peninsula tropospheric temperatures from 1956 to 1999: a synthesis of observations and reanalysis data. Int J Clim 22:291–310. doi:10.1002/joc.758
Martin JH, Gordon RM, Fitzwater SE (1990) Iron in Antarctic waters. Nature 345:156–158. doi:10.1038/345156a0
McKenzie RL, Aucamp PJ, Bais AF, Björnd LO, Ilyas M (2007) Changes in biologically-active ultraviolet radiation reaching the Earth's surface. Photochem Photobiol Sci 6:218–231. doi:10.1039/b700017k
Menden-Deuer S, Lessard EJ (2000) Carbon to volume relationships for dinoflagellates, diatoms, and other protist plankton. Limnol Oceanogr 45:569–579
Metzl N (2009) Decadal increase of oceanic carbon dioxide in Southern Indian Ocean surface waters (1991–2007). Deep Sea Res (II Top Stud Oceanogr) 56:607–619
Mitchell BG, Holm-Hansen O (1991) Bio-optical properties of Antarctic Peninsula waters: differentiation from temperate ocean models. Deep Sea Res (I Oceanogr Res Pap) 38:1009–1028. doi:10.1016/0198-0149(91)90094-V
Moline MA, Prézelin BB (1996) Long-term monitoring and analyses of physical factors regulating variability in coastal Antarctic phytoplankton biomass, in situ productivity and taxonomic composition over subseasonal, seasonal and interannual time scales. Mar Ecol Prog Ser 145:143–160. doi:10.3354/meps145143
Montagnes DJS, Berges JA, Harrison PJ, Taylor FJR (1994) Estimating carbon, nitrogen, protein, and chlorophyll a from volume in marine phytoplankton. Limnol Oceanogr 39:1044–1060
Morán XAG, Estrada M, Gasol JM, Pedrós-Alió C (2002) Dissolved primary production and the strength of phytoplankton-bacterioplankton coupling in contrasting marine regions. Microb Ecol 44:217–223. doi:10.1007/s00248-002-1026-z
Morán XAG, Sebastián M, Pedrós-Alió C, Estrada M (2006) Response of Southern Ocean phytoplankton and bacterioplankton production to short-term experimental warming. Limnol Oceanogr 51:1791–1800
Morel A (1991) Light and marine photosynthesis: a spectral model with geochemical and climatological implications. Prog Oceanogr 26:263–306. doi:10.1016/0079-6611(91)90004-6
Mostajir B, Demers S, De Mora S, Belzile C, Chanut JP, Gosselin M, Roy S, Villegas PZ, Fauchot J, Bouchard J, Bird D, Monfort P, Levasseur M (1999) Experimental test of the effect of ultraviolet-B radiation in a planktonic community. Limnol Oceanogr 44:586–596
Murray AE, Preston CM, Massana R, Taylor LT, Blakis A, Wu K, Delong EF (1998) Seasonal and spatial variability of bacterial and archaeal assemblages in the Coastal Waters near Anvers Island, Antarctica. Appl Environ Microbiol 64:2585–2595
Neale PJ, Talling JF, Heaney SI, Reynolds CS, Lund JWG (1991) Long time series from the English Lake District: irradiance-dependent phytoplankton dynamics during the spring maximum. Limnol Oceanogr 36:751–760
Neale PJ, Cullen JJ, Davis RF (1998) Inhibition of marine photosynthesis by ultraviolet radiation: variable sensitivity of pytoplankton in the Weddell-Scotia Confluence during the austral spring. Limnol Oceanogr 43:433–448
Neale PJ, Helbling EW, Zagarese HE (2003) Modulation of UVR exposure and effects by vertical mixing and advection. In: Helbling EW, Zagarese H (eds) UV effects in aquatic organisms and ecosystems. The Royal Society of Chemistry, Cambridge, pp 107–134
Pearce I, Davidson AT, Bell EM, Wright S (2007) Seasonal changes in the concentration and metabolic activity of bacteria and viruses at an Antarctic coastal site. Aquat Microb Ecol 47:11–23. doi:10.3354/ame047011
Pearce I, Davidson AT, Wright S, Van Den Enden R (2008) Seasonal changes in phytoplankton growth and microzooplankton grazing at an Antarctic coastal site. Aquat Microb Ecol 50:157–167. doi:10.3354/ame01149
Perreault NN, Andersen DT, Pollard WH, Greer CW, Whyte LG (2007) Characterization of the prokaryotic diversity in cold saline perennial springs of the Canadian high Arctic. Appl Environ Microbiol 73:1532–1543
Reiss CS, Hewes CD, Holm-Hansen O (2009) Influence of atmospheric teleconnections and Upper Circumpolar Deep Water on phytoplankton biomass around Elephant Island, Antarctica. Mar Ecol Prog Ser 377:51–62. doi:10.3354/meps07840
Sabatini M, Reta R, Matano R (2004) Circulation and zooplankton biomass distribution over the southern Patagonian shelf during late summer. Cont Shelf Res 24:1359–1373
Sarmiento JL, Slater R, Barber R, Bopp L, Doney SC, Hirst AC, Kleypas J, Matear R, Mikolajewicz U, Monfray P, Soldatov V, Spall SA, Stouffer R (2004) Response of ocean ecosystems to climate warming. Global Biogeochem Cy 18:GB3003. doi:10.1029/2003GB002134
Schäfer H, Muyzer G (2001) Denaturing gradient gel electrophoresis in marine microbial ecology. In: Paul J (ed) Methods in microbiology. Academic Press, London, pp 425–468
Schloss IR, Gustavo AF, Ferrario ME, Almandoz GO, Codina R, Alejandro AB, Balestrini CF, Ochoa HA, Pino DR, Poisson A (2007) Role of plankton communities in sea-air differences in pCO2 in the SW Atlantic Ocean. Mar Ecol Prog Ser 332:93–106. doi:10.3354/meps332093
Setlow RB (1974) The wavelengths in sunlight effective in producing skin cancer: a theoretical analysis. Proc National Acad Sci 71:3363–3366
Siegel V, Loeb V (1995) Recruitment of Antarctic krill *Euphausia superba* and possible causes for its variability. Mar Ecol Prog Ser 123:45–56
Simpson JH (1981) The shelf-sea fronts: implications of their existence and behaviour. Philos Trans R Soc Lond Ser A Math Phys Sci 302:531–546. doi:10.1098/rsta.1981.0181
Smith RC, Baker KS, Stammerjohn SE (1998) Exploring sea ice indexes for polar ecosystem studies. Bioscience 48:83–93. doi:10.2307/1313133

Smith RC, Baker KS, Dierssen HM, Stammerjohn SE, Vernet M (2001) Variability of primary production in an antarctic marine ecosystem as estimated using a multi-scale sampling strategy. Am Zool 41:40–56. doi:10.1093/icb/41.1.40

Smith RC, Martinson DG, Stammerjohn SE, Iannuzzi RA, Ireson K (2008) Bellingshausen and western Antarctic Peninsula region: pigment biomass and sea-ice spatial/temporal distributions and interannual variability. Deep Sea Res (II Top Stud Oceanogr) 55:1949–1963. doi:10.1016/j.dsr2.2008.04.027

Stammerjohn SE, Martinson DG, Smith RC, Iannuzzi RA (2008) Sea ice in the western Antarctic Peninsula region: spatio-temporal variability from ecological and climate change perspectives. Deep Sea Res (II Top Stud Oceanogr) 55:2041–2058. doi:10.1016/j.dsr2.2008.04.026

Takahashi T, Sutherland SC, Sweeney C, Poisson A, Metzl N, Tilbrook B, Bates N, Wanninkhof R, Feely RA, Sabine C, Olafsson J, Nojiri Y (2002) Global sea-air CO_2 flux based on climatological surface ocean pCO_2, and seasonal biological and temperature effects. Deep Sea Res (II Top Stud Oceanogr) 49:1601–1622

Takahashi T, Sutherland SC, Wanninkhof R, Sweeney C, Feely RA, Chipman DW, Hales B, Friederich G, Chavez F, Sabine C, Watson A, Bakker DCE, Schuster U, Metzl N, Yoshikawa-Inoue H, Ishii M, Midorikawa T, Nojiri Y, Körtzinger A, Steinhoff T, Hoppema M, Olafsson J, Arnarson TS, Tilbrook B, Johannessen T, Olsen A, Bellerby R, Wong CS, Delille B, Bates NR, de Baar HJW (2009) Climatological mean and decadal change in surface ocean pCO_2, and net sea-air CO_2 flux over the global oceans. Deep Sea Res (II Top Stud Oceanogr) 56:554–577

Tarran GA, Heywood JL, Zubkov MV (2006) Latitudinal changes in the standing stocks of nano- and picoeukaryotic phytoplankton in the Atlantic Ocean. Deep Sea Res (II Top Stud Oceanogr) 53:1516–1529. doi:10.1016/j.dsr2.2006.05.004

Thomson RE, Fine IV (2003) Estimating mixed layer depth from oceanic profile data. J Atmos Ocean Technol 20:319–329. doi:10.1175/1520-0426(2003)020<0319:EMLDFO>2.0.CO;2

Turner J, Colwell SR, Marshall GJ, Lachlan-Cope TA, Carleton AM, Jones PD, Lagun V, Reid PA, Iagovkina S (2005) Antarctic climate change during the last 50 years. Int J Clim 25:279–294. doi:10.1002/joc.1130

Vaqué D, Guixa-Boixereu N, Gasol JM, Pedrós-Alió C (2002) Distribution of microbial biomass and importance of protists in regulating prokaryotic assemblages in three areas close to the Antarctic Peninsula in spring and summer 1995/96. Deep Sea Res (II Top Stud Oceanogr) 49:847–867. doi:10.1016/S0967-0645(01)00127-8

Vernet M, Martinson D, Iannuzzi R, Stammerjohn S, Kozlowski W, Sines K, Smith R, Garibotti I (2008) Primary production within the sea-ice zone west of the Antarctic Peninsula: I—Sea ice, summer mixed layer, and irradiance. Deep Sea Res (II Top Stud Oceanogr) 55:2068–2085. doi:10.1016/j.dsr2.2008.05.021

Villafañe V, Helbling EW, Holm-Hansen O (1993) Phytoplankton around Elephant Island, Antarctica, distribution, biomass and composition. Polar Biol 13:183–191. doi:10.1007/BF00238928

Wang X, Yang G-P, López D, Ferreyra G, Lemarchand K, Xie H (2009) Late austral autumn to spring evolutions of water-column dissolved inorganic and organic carbon in the Scholaert Channel, West Antarctic. Antarct Sci. doi:10.1017/S0954102009990666

Xenopoulos MA, Prairie YT, Bird DF (2000) Influence of ultraviolet-B radiation, stratospheric ozone variability, and thermal stratification on the phytoplankton biomass dynamics in a mesohumic lake. Can J Fish Aquat Sci 57:600–609. doi:10.1139/cjfas-57-3-600

Zapata M, Rodríguez F, Garrido JL (2000) Separation of chlorophylls and carotenoids from marine phytoplankton: a new HPLC method using a reversed phase C8 column and pyridine containing mobile phases. Mar Ecol Prog Ser 195:29–45. doi:10.3354/meps195029

Zubkov MV, Sleigh MA, Burkill PH (2000a) Assaying picoplankton distribution by flow cytometry of underway samples collected along a meridional transect across the Atlantic Ocean. Aquat Microb Ecol 21:13–20. doi:10.3354/ame021013

Zubkov MV, Sleigh MA, Burkill PH, Leakey RJG (2000b) Picoplankton community structure on the Atlantic Meridional Transect: a comparison between seasons. Prog Oceanogr 45:369–386. doi:10.1016/S0079-6611(00)00008-2